22. Manning, F. S., and L. N. Canjar, *J. Chem. Eng. Data*, **6**, 364 (1961).
23. Mather, A. E., V. F. Yesavage, J. E. Powers, and D. L. *Ktaz, Proc. Ann. Conv., Natl. Gas Process. Assoc., Tech. Papers*, **45**, 12 (1966).
24. *Ibid.*, **46**, 8 (1967).
25. Mather, A. E., J. E. Powers, and D. L. Katz, paper presented at *IUPAC Symp. Thermodynamics*, Heidelberg, Germany (Sept. 12, 1967).
26. ———, Ph.D. thesis, The Univ. of Michigan, Ann Arbor (1967).
27. Reamer, H. H., B. H. Sage, and W. N. Lacey, *Ind. Eng. Chem.*, **42**, 534 (1950).
28. Roebuck, J. R., *Phys. Rev.*, (2), **2**, 299 (1913).
29. ———, *Proc. Am. Acad. Arts. Sci.*, **60**, 537 (1925).
30. ———, and H. Osterberg, *Phys. Rev.*, **48**, 450 (1935).
31. Stotler, H. H., and M. Benedict, *Chem. Eng. Prog. Symp. Ser. No. 6*, **49**, 25 (1953).
32. Stribolt, K. Ö., and A. Lydersen, *Chem. Ing. Tech.*, **39**, 96, (1967).
33. Yarborough, L., and W. C. Edmister, *AIChE J.*, **11**, 492 (1965).
34. Yen, L. C., personal communication (Apr. 24, 1967).

Manuscript received November 1, 1967; revision received December 26, 1967; paper accepted January 7, 1968. Paper presented at AIChE New York meeting.

Oxidation of Hydrogen in a Helium Stream by Copper Oxide: Analysis of Combined Film and Pore Diffusion with Rapid Irreversible Reaction in a Fixed-Bed Process

CHARLES D. SCOTT

Oak Ridge National Laboratory, Oak Ridge, Tennessee

Differential equations were derived to describe the system characterized by a rapid, irreversible reaction of a fluid species in a flowing fluid with a fixed bed of solids in which the reaction rate was controlled by mass transfer of the reacting fluid from the bulk fluid to the reaction site in the solid. Two kinds of mass transfer resistances were assumed, external or film diffusion resistance, and internal pore diffusion resistance. The set of differential equations were solved by a finite-difference method for both the generalized case and for the specific case of reaction of hydrogen in a stream of helium with fixed beds of copper oxide pellets.

The hydrogen-copper oxide reaction is one step in a proposed method for removal of hydrogen as a contaminant in the helium coolant of nuclear reactors. This reaction was experimentally investigated in tests with both differential and deep beds of copper oxide in the temperature range of 400 to 600°C., at pressures of 10.2 to 30.0 atm., with gas mass flow rates of 0.0050 to 0.050 g./sq.cm.-sec, and with inlet hydrogen concentrations of 0.0008 to 1.21 vol. %. These tests showed that the system could be described by the two rate-limiting steps: film and pore diffusion of hydrogen. Differential-bed tests were used to establish hydrogen transport properties within the porous copper oxide pellets, and tests with deep beds were used to establish external mass transport properties.

Generalized breakthrough curves were determined by a computer solution of the mathematical model. These curves can be the basis for design of fixed-bed copper oxide oxidizers for gas-cooled, nuclear reactor purification systems and for design of any fixed-bed system which follows the assumed reaction mechanism.

Hydrogen is one of the major nonradioactive contaminants expected in the helium coolant of gas-cooled nuclear reactors. The hydrogen content of the coolant must be kept at a reasonably low level to maintain a coolant of acceptable properties. A proposed method for removing hydrogen from the helium is a two step process in which the hydrogen is first oxidized to water which is then removed by sorption (*1*). One oxidizing system that can be used is a fixed bed of copper oxide pellets, which can be alternately depleted of its oxygen content by reaction with hydrogen (copper oxide + hydrogen = copper + water) and then regenerated by air or oxygen (copper + $1/2O_2$ = copper oxide). In accordance with anticipated requirements for gas-cooled nuclear reactors, the ranges of operating conditions of interest are pressure, 10 to 30 atm.; temperature, 400 to 600°C., contamination level, 0.001 to 1.0 vol.%; gas mass flow rate, 0.005 to 0.050 g./sq.cm.-sec.

Knowledge of the effects of various system parameters on the rate of the reaction is needed so that fixed bed, copper oxide oxidizers for helium purification systems can be designed. The approach taken in this study was to first establish the reaction mechanism for the hydrogen-copper oxide system and then by a mathematical model of the system to predict behavior of the copper oxide bed for the range of anticipated operating conditions. The mathematical solution was extended to the general case, which is useful for any fixed-bed system with porous solids in which a rapid, irreversible reaction occurs and in which the rate of reaction is controlled by the mass transfer of the reacting fluid species from the flowing fluid to the solid reaction site.

PREVIOUS WORK

Hydrogen-Copper Oxide Reaction

The kinetics of the hydrogen-copper oxide reaction in static systems has already been studied by several investigators (*9, 21, 25, 26, 38*). They found that at temperatures less than 200°C. the reaction was preceded by an incubation period, which was attributed to the autocatalytic effect of reduced copper. At higher temperatures, the autocatalytic effect was less significant, and mass transport effects were noted. Bond and Clark (*2*), in using a flow system, noted flow-rate effects on the reaction rate when fixed beds of copper oxide were contacted by hydrogen-argon mixtures at 300°C. These mass transfer effects were also noticed in this study.

Fixed-Bed Operation

The problem of the transfer of heat or mass from a flowing fluid to a fixed bed of solids has been the subject of a large amount of literature both from the experimental and mathematical viewpoints. Of particular interest for this study is the mathematical representation of the fixed-bed operation in which the rate of mass transfer is controlled by diffusional processes both external to the solid phase and within the solid itself. Excellent surveys of such mathematical treatments have been presented by Thiele (*32*), Klotz (*20*), and Vermeulen (*34*).

Most of the reported work is for ion exchange or sorption processes in which a linear isotherm is assumed to exist. Solutions for the fixed-bed effluent concentration of the reactant as a function of time have been derived by Rosen (*30*), Kasten et al. (*19*), and Masamune and Smith (*23*) for linear isotherms; and Vermeulen (*33*) has presented an approximate solution for the irreversible reaction with both gas phase and intraparticle diffusion.

Film Diffusion

The gas-phase resistance to mass transfer of a gas species to a solid surface is usually represented by a gas film surrounding the solid through which the reacting species must diffuse. Such mass transfer processes are described by the dimensionless mass transfer factor J_D of Chilton and Colburn (*7*), which can be expressed in terms of the mass transfer coefficient, Schmidt number, and physical properties of the fluid:

$$J_D = (k\rho/G)(N_{Sc})^{2/3} \qquad (1)$$

The mass tranfer factor is generally correlated as a function of the modified Reynolds Number, N_{Re}. Such workers as Gaffney and Drew (*13*), Hobson and Thodos (*16*), Carberry (*6*), Bradshaw and Bennet (*5*), and several others were able to correlate a large amount of mass transport data in this way.

In such correlations, there has been some disagreement on the effects of Reynolds number (*8, 11*) and fluid properties (*31*). Resnick and White (*29*) and Hurt (*18*) felt that they showed an effect of particle size on the mass transfer factor; however, Ergun (*12*) has questioned the results of the former and he showed how the effect of particle size could be incorporated into a unified correlation.

Pellet-Phase Diffusion

The pellet-phase mass transfer of fluid with a rapid, irreversible reaction with the solid has been considered by several workers. Hermans (*15*) showed that a sharp reaction boundary within the solid was necessary. Levenspiel (*22*) and others mathematically treated a model in which diffusion through a nonreactive layer controlled the rate of reaction and Weiss and Goodwin (*36*) experimentally verified a similar shell-progressive model. Others (*4, 27*) showed that a mathematical solution might be possible by a pseudo steady state approximation if the fluid concentration of the reacting species was small compared with the solid phase concentration. Bischoff (*3*) showed that this approximation would be valid for most gas-solid systems.

Observed diffusion rates of gases through porous solids are less than those predicted by assuming that all pores are straight circular pores with the same area and volume as the internal pellet area and void volume. This has been attributed to tortuosity of the pores and is compensated for by tortuosity factors (*17, 37*) or by the determination of an effective porosity or effective diffusivity in the porous solid (*14, 35*).

THEORETICAL CONSIDERATIONS

The copper oxide pellets used in this study were in the form of short cylinders whose lengths were approximately equal to their diameters. To treat this system mathematically a reasonably simple geometrical shape (that is, either a sphere or an infinite cylinder) must be assumed. The pellet's volume and shape could be closely approximated by a sphere of equivalent volume. Such an assumed shape had a major dimension and total surface area within 13% of the actual pellet. Use of an infinite cylinder for the approximation could not approach this fit and the additional mathematical complexities of other geometrical shapes make them unusable.

Consider a fixed bed of such pellets in which a fluid stream containing a contaminant which can react with the solid, flows through the bed. Reaction will occur during the transit of the fluid through the bed. If physical properties are assumed constant, if plug flow is assumed, if the concentration of reacting species is small, and if diffusion in the direction of flow is negligible, then the concentration of the contaminant in the external void space in the fixed bed can be described by (*20*):

$$\left(\frac{\partial C}{\partial t}\right)_z + (u)\left(\frac{\partial C}{\partial z}\right)_t = -\frac{1}{\epsilon}\left(\frac{\partial n}{\partial t}\right)_z \qquad (2)$$

The solution of Equation (2) depends on the mathematical relation one uses for the local rate of removal of the contaminant by the solids $(\partial n/\partial t)_z$. The particular mathematical form depends on the proposed mechanism of the removal process. For the case of a rapid and irreversible reaction at the reaction site, mass transfer of the contaminant to the reaction site from the bulk gas stream is the rate-controlling mechanism. Such a mechanism would demand that a partially reduced pellet should have a well defined reaction interface in a spherical shell and that the reacting species would have to diffuse through the reacted phase to reach the reaction site.

The resistance to mass transport from the bulk gas to the reaction site can be described by an external film resistance and an internal resistance due to pore diffusion of the contaminant (hydrogen). This results in a physical model (Figure 1) in which the sphere of radius r_E is surrounded by a gas film in which a certain portion of the porous sphere has already been reacted, r_I to r_E, and finally there is an unreacted portion enclosed by a spherical shell at a radius of r_I.

The gas phase contaminant concentration will be some value C_E at the pellet surface; there will be a gas phase concentration gradient within the reacted phase of the pellet due to the pore diffusion; and the contaminant gas concentration at and inside the reaction interface will be zero.

If the radial diffusion is governed by Fick's Law, and if the reaction interface r_I moves slowly (low contaminant concentration), the diffusion of the contaminant will pro-

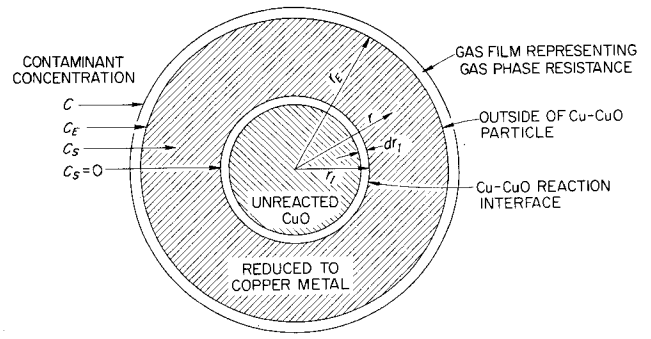

Fig. 1. Physical model used to describe the case of a rapid, irreversible reaction with rate controlled by gas phase and pellet phase diffusion.

ceed essentially at steady state for a small increment of time. For such a case, Crank (*10*) showed:

$$\left(\frac{\partial^2 U}{\partial r^2}\right)_t = 0 \tag{3}$$

where the variable U is defined as $U(C_s, r) = C_s \cdot r$, which is subject to the boundary conditions:

$$U(C_s, r_E) = C_E r_E$$
$$U(C_s, 0) = 0$$

Solution of Equation (3) with these boundary conditions gives:

$$C_s = \frac{C_E r_E}{r}\left(\frac{r - r_I}{r_E - r_I}\right) \tag{4}$$

The external resistance to mass transport of the contaminant can be represented by diffusion across a stagnant gas film surrounding the solid sphere where the rate of transport is described by:

$$\left(\frac{\partial n}{\partial t}\right)_z = ka(C - C_E) \tag{5}$$

Also, this rate of transport at the external surface must be equal to the rate of internal contaminant transport to the reaction interface (assuming negligible holdup in the sphere):

$$\left(\frac{\partial n}{\partial t}\right)_z = \frac{4\pi\alpha D\tau r_I r_E C_E}{r_E - r_I} \tag{6}$$

The combination of Equations (5) and (6) gives an expression independent of C_E:

$$\left(\frac{\partial n}{\partial t}\right)_z = \frac{4\pi\alpha D\tau kar_E r_I C}{4\pi\alpha D\tau r_E r_I + ka(r_E - r_I)} \tag{7}$$

This gives the specific reaction rate as a function of bulk-gas contaminant concentration and the position of the reaction interface r_I. But, r_I is also a variable, and an expression for the movement of the interface is needed for a complete solution. Comparing the rate of reaction with the necessary movement of the reaction interface gives:

$$\left(\frac{\partial r_I}{\partial t}\right)_z = -\frac{1}{4\pi b r_I^2 \tau}\left(\frac{\partial n}{\partial t}\right)_z \tag{8}$$

The reaction system is now completely described by Equations (2), (7), and (8).

A more general form of these equations can be obtained by a change in variables. Vermeulen showed that use of the dimensionless variables (*34*),

$Z = 3C_o(Ft - v\epsilon)/\pi 4 r_E^3 b\tau v$, dimensionless throughput parameter
$X = C/C_o$, dimensionless fluid-phase concentration
$Y = n/[4/3(\pi r_E^3 b\tau)]$, dimensionless pellet-phase concentration
$V = v/v_t$, dimensionless bed volume
$R = r/r_E$, dimensionless pellet radius

in Equations (2), (7), and (8), results in:

$$\left(\frac{\partial X}{\partial V}\right)_{ZV} = -\left(\frac{\partial Y}{\partial ZV}\right)_V \tag{9}$$

$$\left(\frac{\partial Y}{\partial ZV}\right)_V = \frac{kav_t X}{F}\left[\frac{4\pi\alpha D r_E R_I \tau}{4\pi\alpha D r_E R_I \tau + ka(1 - R_E)}\right] \tag{10}$$

and

$$\left(\frac{\partial R_I}{\partial ZV}\right)_V = -\frac{1}{3R_I^2}\left(\frac{\partial Y}{\partial ZV}\right)_V \tag{11}$$

Further, defining dimensionless transport properties,

$K_E = kav_t/F$, dimensionless external mass transport property
$K_I = 4\pi\alpha D\tau r_E v_t/F$, dimensionless internal mass transport property

and substituting into Equation (10) gives:

$$\left(\frac{\partial Y}{\partial ZV}\right)_V = K_E X\left[\frac{K_I R_I}{K_I R_I + K_E(1 - R_I)}\right] \tag{12}$$

Equations (9), (11), and (12) are the three dimensionless differential equations that define the system, and the two parameters K_E and K_I represent the mass transport properties of the fluid contaminant. These equations may be solved simultaneously by finite-difference methods on a high speed digital computer.

EXPERIMENTAL PROCEDURE

Two types of kinetic tests were made, differential-bed tests in which monolayers of copper oxide pellets were used and deep-bed tests in which bed volumes of 24.2 cc. (1.27 cm. bed depth) to 291.0 cc. (15.24 cm. bed depth) were used. These tests allowed establishment of the kinetic model of the reaction system and consequently allowed determination of the transport properties of hydrogen across the gas film and through the porous solid.

Materials

The copper oxide pellets were in the form of compacted, right circular cylinders. After being sintered in air at 1,000°C.

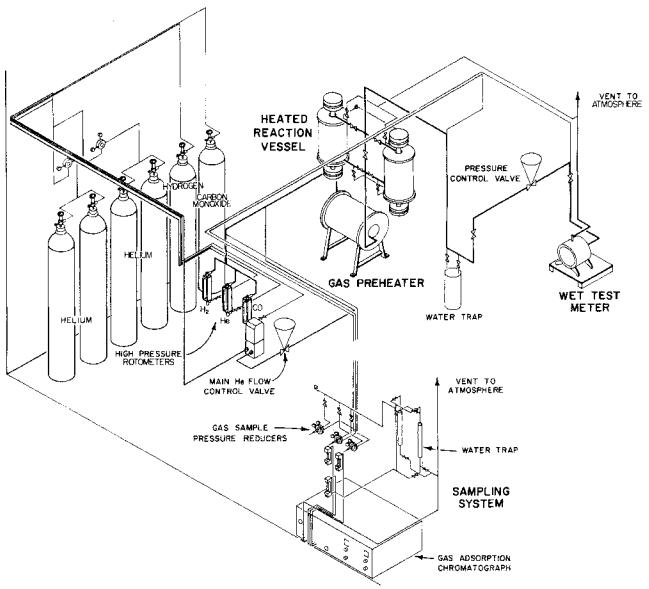

Fig. 2. Experimental facility.

for 8 to 16 hr. to remove residual carbon and establish size stability, the pellets typically had dimensions of 0.095 in. diam. × 0.096 in. specific surface area of 0.68 sq. m./g., a carbon content of < 0.15%, a total porosity of about 0.30, a tap density of 3.1 g./cc., and a most probable pore radius of 0.14μ (as determined by mercury intrusion and nitrogen adsorption).

The two gases, helium and hydrogen, used in the experiments were more than 99.95 and 99.5% pure, respectively.

Equipment

The apparatus was composed of a gas metering and heating section, reaction vessels, and a gas analysis section (Figure 2). The main helium stream was metered by an instrumented orifice meter, and the hydrogen flow by a high-pressure rotameter. The two gases were then introduced into a common line, preheated in tube furnaces, and introduced to 5 cm. I.D., stainless steel reaction vessels. Each reactor was externally heated and insulated by a tube furnace, and each was internally insulated at the ends. Internal reactor temperatures and reactor wall temperatures were measured to ± 1°C. by thermocouples. Internal reactor and adjacent wall temperatures were maintained to within ± 2°C. to prevent large errors due to radiation losses.

System pressure was controlled in the range 10 to 30 atm. by a pneumatic controller connected to a pressure-sensing cell and control valve, and the gas sampling and analysis portion of the system was composed of a gas-adsorption chromatograph with connections to the gas stream both before and after the reaction vessels. A small side stream of the gas was allowed to pass through the sampling system continuously, and periodic samples could be taken from the gas stream for the chromatograph. The sensing devices in the chromatograph were two thermal-conductivity cells used to determine the hydrogen concentration by comparative thermal conductivity of a reference gas stream, either helium or argon, and a carrier gas stream, either helium or argon, into which portions of the contaminated helium was injected automatically and periodically. Calcium sulfate was used to dry the gas stream prior to its entry into the chromatograph, and type 5-A Linde molecular sieves were used in the adsorption column.

Differential-Bed Tests

For differential-bed tests, the effective reactor diameter was decreased to ~1.25 cm. by placing a stainless steel insert in its center and the gas flow rate was increased to its maximum value (Figure 3). This increased the gas velocity significantly and tended to decrease the effects of gas-phase film diffusion. The latter was further verified by decreasing the gas velocity by a factor of two and noting no appreciable change in the rate of reaction. A monolayer of copper oxide pellets (10 to 15 pellets) was loaded into the stainless steel insert on top

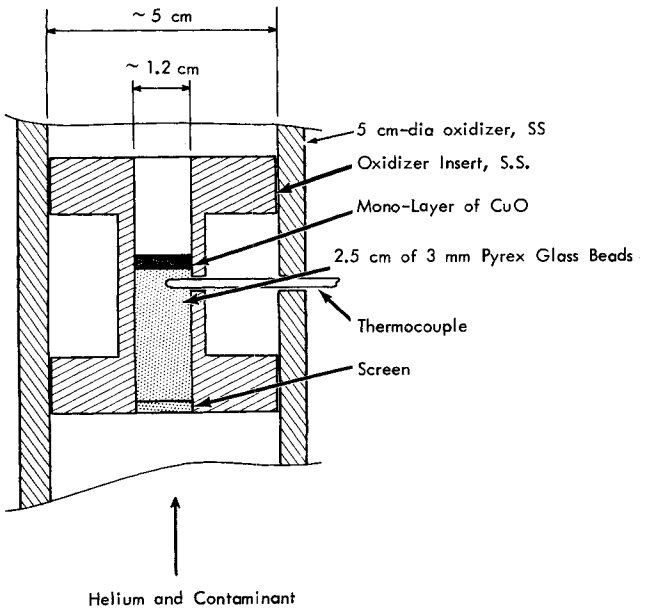

Fig. 3. Apparatus for differential-bed tests.

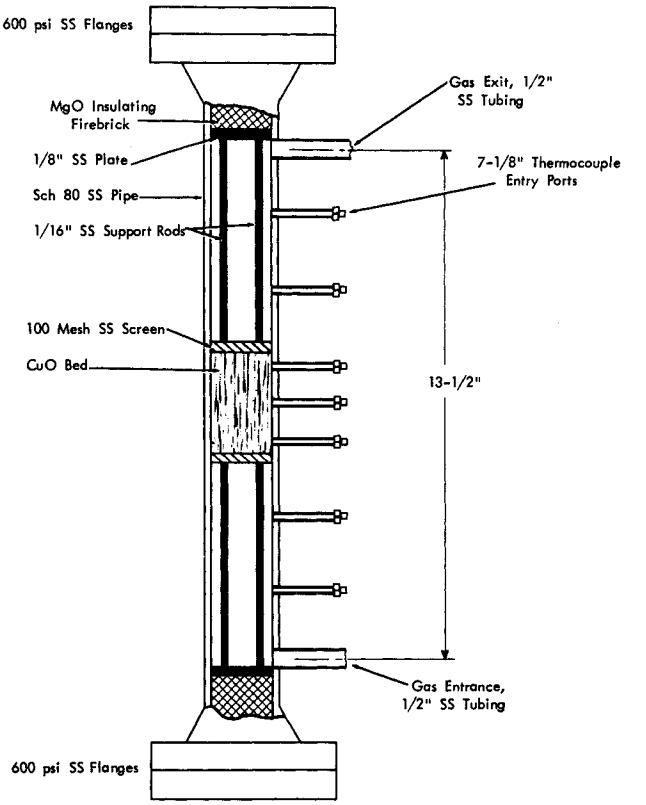

Fig. 4. Reaction vessel without external heater.

of a 2.5 cm. depth of 3 mm. Pyrex glass beads and a thermocouple was inserted in the reaction zone just below the differential bed.

Each differential-bed test was made by first initiating and maintaining a constant flow of preheated helium through the heated oxidizer until thermal equilibrium was established. Hydrogen was then introduced to the helium stream at a constant rate for a specific length of time, and the effluent gas stream was periodically analyzed by the chromatograph for its hydrogen content. After each run, the differential bed was cooled under an inert atmosphere and removed at room temperature. The bed of copper oxide pellets was removed and weighed, and the individual pellets of copper-copper oxide were sectioned by a belt sander, partially polished by fine emery paper, etched in dilute nitric acid, and observed by an optical microscope. Twenty-three differential-bed tests were made in the range of 400 to 600°C., 10.2 to 30 atm. pressure, and 0.0008 to 1.08% hydrogen.

Deep-Bed Tests

The full reactor diameter, 5.0 cm., was used for deep-bed tests. The reactor was charged with copper oxide pellets, and a 5 cm. depth of 3 mm. Pyrex glass beads was placed on the top and the bottom of the copper oxide bed to smooth out entrance and exit conditions (Figure 4). The reactor was heated to the desired operating temperature, and hydrogen was introduced after reaching thermal equilibrium with a preheated stream of pure helium. A sidestream was continuously removed from the reaction vessel effluent stream and sent to the gas sampling system. Every 6 to 20 min., 5 cc. of this sidestream was injected into the carrier stream of the chromatograph for hydrogen determination. Twenty-eight deep-bed tests were made in the range of 400 to 600°C., 10.2 to 30 atm. pressure, 24.3 to 291.0 cc. copper oxide, gas flow rate of 35.3 to 228.0 standard liters/min., and hydrogen concentration of 0.011 to 1.24%.

No attempt was made to measure the uniformity of mass flow rate as a function of radial position; however, the total mass flow rate was maintained within ± 5% of the average flow rate.

ANALYSIS OF RESULTS

The results of the experiment were used to establish re-

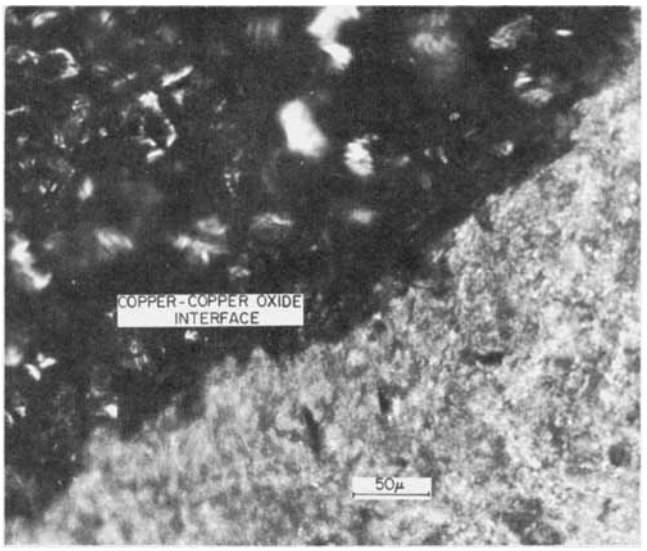

Fig. 5. Sectioned copper oxide pellet that has been partially reduced.

action mechanism and to validate the assumed model of the reaction system. When partially reacted copper oxide pellets were sectioned, a well-defined copper-copper oxide interface was observed in each pellet (Figure 5). Such an interface would be necessary if the mechanism of reaction control within the pellets was by mass transport of the hydrogen from the external surface to the reaction side. Since the pellets were relatively porous, and since the pores were large, the mechanism for such transport would probably be pore diffusion of the hydrogen. The requirement of an irreversible reaction at the reaction side was satisfied since the free energy of the hydrogen-copper oxide reaction is approximately −30 k.cal. in the range of conditions of interest.

Pellet Phase Mass Transport Property

The experimental results of the differential-bed tests were used to determine the type of mass transport and the effective porosity in the reduced copper oxide pellets. To determine the effective porosity, the type of hydrogen transport expected within the pellet was first established. Since the pores within the copper oxide pellets are significantly larger than the mean free path of hydrogen in the range of conditions of interest (at 500°C. and 20 atm., the mean free path of hydrogen is approximately 2×10^{-6} cm., and the pore radii ranged from approximately 1 to 5×10^{-5} cm.), it is safe to assume that transport of the hydrogen within the pellet is by molecular diffusion through the pores. Molecular diffusion of hydrogen in helium within the pores of the pellet can be determined from available correlations; however, to completely characterize the pellet phase hydrogen mass transport, the fraction of radial area available for transport must be known. This can be approximated by an effective porosity for mass transport. The effective porosity should be constant for all sets of operating conditions, and it should be less than the total porosity since all available void volume or pores in the pellet do not lead radially to the reaction shell.

A material balance written around the reaction interface within a spherical pellet which equates the rate of diffusion of hydrogen to the movement of the interface due to reaction after rearrangement becomes (22):

$$\left(r_I - \frac{r_I^2}{r_E}\right) dr_I = -\frac{\alpha D C_E}{b}\, dt \qquad (13)$$

At the conditions of the differential-bed tests where film diffusion was apparently not significant and the bulk gas concentration of hydrogen was essentially constant, Equation (13) can be integrated to give an expression for the effective porosity:

$$\alpha = \frac{b}{DCt}\left(\frac{r_E^2}{6} + \frac{r_I^3}{3r_E} - \frac{r_I^2}{2}\right) \qquad (14)$$

If cylindrical geometry (cylindrical pellets of infinite length) had been used in the mathematical treatment, the resulting equation for the effective porosity would be

$$\alpha = \frac{b}{DCt}\left(\frac{r_I^2}{2}\ln\frac{r_I}{r_E} + \frac{r_E^2 - r_I^2}{4}\right) \qquad (15)$$

To account for the nonuniformity of the pellets in each run, the term

$$A = \left(\frac{r_E^2}{6} + \frac{r_I^3}{3r_E} - \frac{r_I^2}{2}\right) \qquad (16)$$

was determined for each pellet of each differential-bed test, and an average value of A was used in determination of the average effective porosity for each test.

Empirical correlations of Reid and Sherwood (28) were used to determine the molecular diffusivity of hydrogen in the hydrogen-helium mixtures and the correlations of Massey (24) were used to establish the viscosity and density of the hydrogen-helium mixtures at the conditions of interest.

The effective porosity was fairly constant over the entire range of experimental conditions tested, with an average value of 0.0566 and a standard deviation of 0.0085. Some variation in the effective porosity may be due to nonhomogeneity of the copper oxide pellets, and the small number of pellets used for each test was probably not sufficient to obtain a good statistical average since the individual pellets appear to have a wide range of physical properties.

On the basis of the apparent constancy of the effective porosity, it was concluded that the resistance in the pellet phase to reaction of hydrogen with copper oxide could be

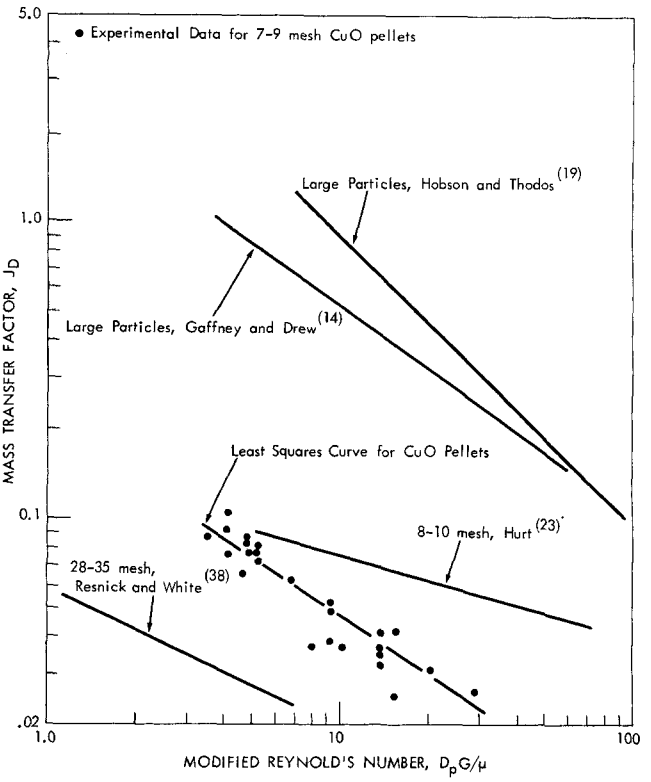

Fig. 6. Mass transfer factor as a function of the modified Reynold's number as determined from deep-bed tests.

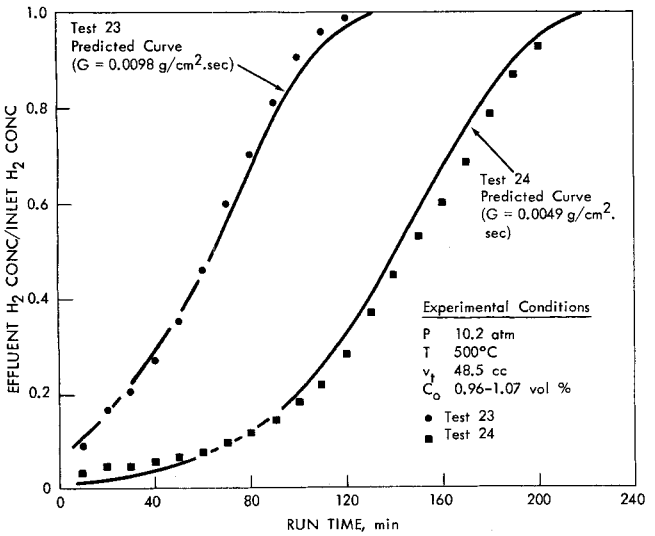

Fig. 7. Effluent hydrogen concentration histories for deep-bed tests 23 and 24 showing the effect of change in mass flow rate and the comparison between experimental and model predicted results.

described by mass transport of the hydrogen to the reaction site by molecular diffusion through pores in the pellet. Obviously, some resistance to hydrogen transport through the small individual copper oxide particle would be expected; however, no visual evidence was found of partially reduced copper oxide particles. This probably indicated that the size of the individual particles was small enough to prevent significant resistance to hydrogen transport (average copper oxide particle size was approximately 40 μ).

External Mass Transport Property

The mass transport property for hydrogen diffusion across an external gas film can be presented as the mass transfer coefficient k, used in Equation (5). Values of k can be correlated as a function of the various physical properties of the system, and the usual correlation is the mass transport factor, J_D, as a function of the modified Reynolds number, N_{Re}. Rather than choose one particular published correlation for use in this system, the mass transfer factor was determined for each deep-bed test, and a correlation of mass transfer factor as a function of modified Reynolds number was made.

In the initial phase of deep-bed tests, the major resistance to the mass transfer of hydrogen to the reaction site will be due entirely to the stagnant gas film surrounding the exterior of the copper oxide pellet or to film diffusion of hydrogen. Since the reaction rate of hydrogen with copper oxide is apparently rapid at the reaction site, the concentration of hydrogen at the surface of the pellet at the beginning of the test will be approximately zero. The reaction rate can then be expressed by

$$\left(\frac{\partial n}{\partial t}\right)_z = kaC \tag{17}$$

By substituting Equation (17) into Equation (2), and noting that during the initial phase of this type of reaction the bulk gas phase concentration of the species of interest is not dependent on time:

$$u\left(\frac{dC}{dz}\right) = -\frac{kaC}{\epsilon} \tag{18}$$

Integration of Equation (18) results in

$$\ln\frac{C}{C_o} = -\frac{kaz}{u\epsilon} \tag{19}$$

which is the solution for the gas-phase concentration of hydrogen as a function of bed height. Equation (18) can be rearranged and used to obtain values of k from deep-bed tests,

$$k = \frac{u\epsilon}{az}\ln\frac{C_o}{C} \tag{20}$$

if the effluent concentration is known at the beginning of the run.

The mass transfer coefficient k was determined for each deep-bed test by extrapolating the effluent hydrogen concentration to zero time. J_D was correlated with N_{Re} (Figure 6), and the resulting expression for the least square fitted curve was:

$$J_D = 0.216\,N_{Re}^{-0.67} \tag{21}$$

This correlation is within the range of published correlations and the best agreement is with that of Hurt's data (*18*) although it has been questioned in the past (*12*). The system studied had high pressures and temperatures which might have contributed to the lower J_D values and the effect of particle size is probably a significant factor. It is interesting to note that the slope of the J_D vs. N_{Re} curve is very close to that reported by Gaffney and Drew (*13*).

Deep-Bed Tests

The final means of verifying the assumed mathematical model was to use the experimentally determined hydrogen transport properties of the system (that is, the effective porosity determined from differential bed tests and the external mass transport coefficient from the beginning of the deep bed tests) to predict the hydrogen effluent concentration history curve for each deep-bed test. These predicted curves were then compared with experimental results from deep-bed tests.

The experimental data can be presented as a series of hydrogen concentration history curves, and these same graphs can be used for comparison with the model predicted effluent hydrogen concentration. Figures 7 through 9 are typical of the deep-bed data. They are S shaped curves typical of percolation processes. Figure 7 shows the effect of change in mass flow rate. An increase in gas mass flow rate tends to exhaust the copper oxide bed more rapidly and to make the curves much sharper. An increase in inlet hydrogen concentration also tends to give a much sharper effluent hydrogen concentration history curve (Figure 8). A change in system temperature has little effect on the curves; however, the effects are predictable, and experimental results generally follow predicted results. The effect of change in copper oxide bed volume is shown in Figure 9.

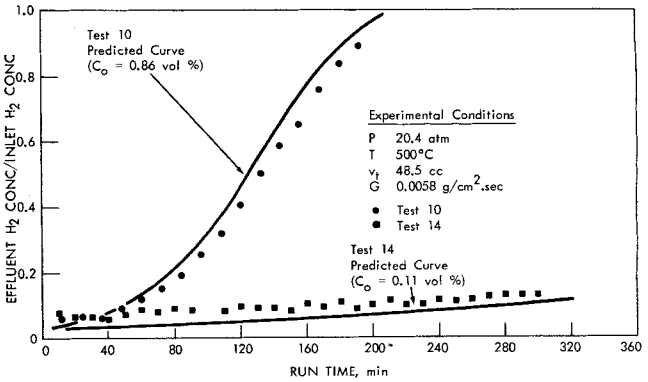

Fig. 8. Effluent hydrogen concentration histories for deep-bed tests 10 and 14, showing the effect of change in hydrogen concentration and the comparison between experimental and model predicted results.

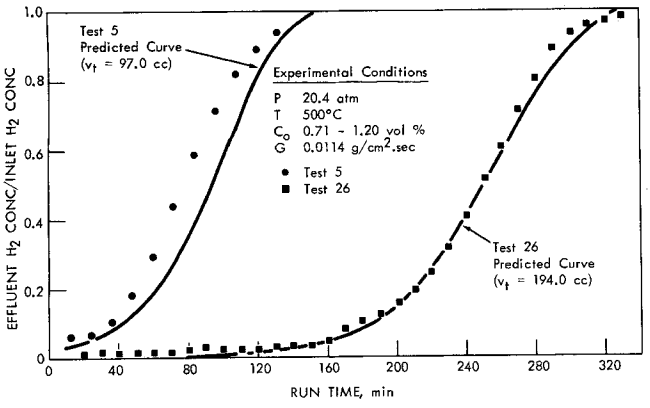

Fig. 9. Effluent hydrogen concentration histories for deep-bed tests 5 and 26, showing the effect of change in copper oxide bed volume and the comparison between experimental and model predicted results.

Agreement between experimental and predicted effluent hydrogen concentration history curves was, in general, good. There was noticeable deviation between the predicted and experimental results in some tests at two points. In some low concentration tests, the initial part of the experimental curve started out somewhat high but decreased after a short time to approximate the predicted results. This initial deviation may have been due to dependence on the autocatalytic effect of the hydrogen-copper oxide reaction, noted by some workers at much lower temperatures but higher hydrogen concentration. For solid phase diffusion resistance in the small copper oxide particles to be a factor, the effluent hydrogen concentration history curve should initially be higher than the predicted curve and then fall below the predicted curve as bed exhaustion is approached. This type of experimental deviation was observed in some tests; however, the deviations were so small that they could also be explained by inaccuracies in experimental technique.

The utility of the generalized or dimensionless mathematical model can be shown by plotting dimensionless effluent concentration history curves for tests made with approximately equal dimensionless mass transport properties. There was reasonable correlation for these dimensionless cases, as shown in Figure 10.

Experimental Error

The hydrogen concentration was measured by a gas-

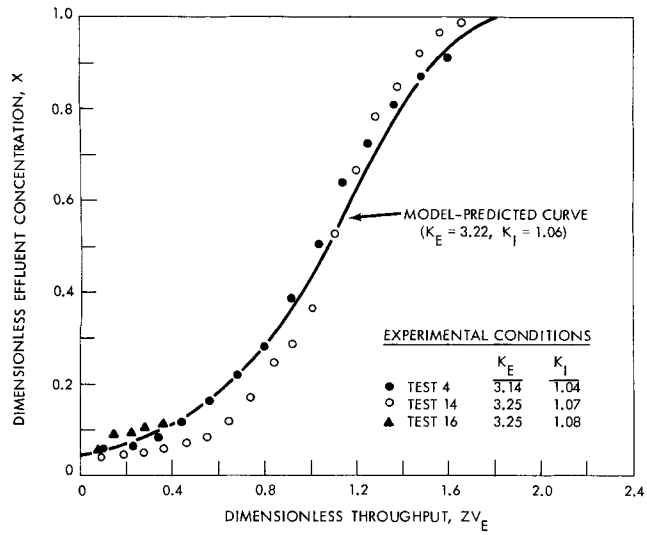

Fig. 10. Correlation of experimental data from tests 4, 14, and 16 by dimensionless variables and comparison with model predicted results for average values of the mass transport properties.

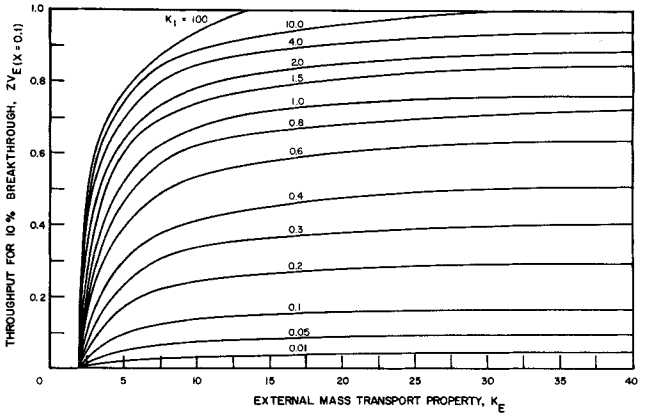

Fig. 11. Model predicted 10% breakthrough as a function of dimensionless mass transport properties.

adsorption chromatograph. This instrument had an accuracy of ± 3% in the range of 0.01 to 1 vol. % hydrogen. The other major experimental error was measurement and maintenance of the gas flow rate. This was measured and controlled within ± 5% of the average flow rate for each run.

In all deep tests, deviation of experimental data from model predicted curves did not exceed limits of these experimental errors, except for the initial deviations at very low hydrogen concentrations noted earlier.

DESIGN CONSIDERATIONS

A series of the generalized breakthrough curves would completely define the system of interest and any other system with similar rate mechanisms. However, the design data can be presented in a single graph if breakthrough is defined as an effluent concentration which is 10% of the inlet concentration. In such a plot (Figure 11) the throughput parameter at 10% breakthrough is presented as a function of K_E for a series of values of K_I.

If a system other than the one reported here is to be considered, one would obviously hav eto first establish that it had a similar reaction rate control and then a sufficient amount of experimental data would have to be obtained to determine the effective porosity and external mass transport properties. As in most cases where a mathematical analysis is the basis for correlation of experimental data, the amount of data needed to describe the system should be significantly less than for a totally empirical correlation.

COMPUTER SOLUTION OF MATHEMATICAL MODEL

The set of differential equations describing the mathematical model of the reaction system can be solved by a finite-difference method. For example in the generalized case, the three defining differential equations, (9), (11), and (12), put in finite difference form became the operating equations for the computer solution. These equations are:

$$X_{m+1,m} = X_{m,n} - \Delta V \left(\frac{\partial Y}{\partial ZV}\right)_{m,n} \tag{22}$$

$$\left(\frac{\partial Y}{\partial ZV}\right)_{m,n} = K_E X_{m,n} \left[1 - \frac{K_E(1 - R_{I,m,n})}{K_I R_{I,m,n} + K_E(1 - R_{I,m,n})}\right] \tag{23}$$

$$\Delta R_{I,m,n} = -\frac{\Delta ZV}{3(R_{I,m,n})^2} \left(\frac{\partial Y}{\partial ZV}\right)_{m,n} \tag{24}$$

where m designates increments of column volume ΔV apart, which are numbered consecutively from the gas in-

let, and n represents increments of ZV measured from the initial values of ZV when time is equal to zero.

The computer code was written for the IBM 7090 digital computer, and, in all computer runs, a ΔV of 0.01 and a ΔZV of 0.001 were used. Reduction of either by a factor of 2 changed the dimensionless effluent hydrogen concentration by $< 1\%$.

ACKNOWLEDGMENT

The author is grateful for the helpful suggestions of Dr. J. J. Perona and Dr. M. E. Whatley of Oak Ridge National Laboratory, and of Dr. H. F. Johnson and Dr. S. H. Jury of the University of Tennessee. The fine technical assistance of W. G. Sission of Oak Ridge National Laboratory is also acknowledged.

This research was sponsored by the U.S. Atomic Energy Commission under contract with Union Carbide Corporation.

NOTATION

a = effective mass transfer area between fluid and copper oxide pellets, sq.cm./cc. of bed
A = $(r_E^2/6 + r_I^3/3r_E - r_I^2/2)$, sq.cmf
b = ultimate amount of the reacting fluid which can be reacted by the pellet phase, g.-mole/cc. of pellet
C = concentration of the reacting fluid in the fluid phase, g.-mole/cc.
d_p = diameter of sphere equal in volume to actual pellet, cm.
D = molecular diffusivity, s.cm./sec.
F = volumetric flow rate, cc./sec.
G = mass flow rate, g./sq.cm. sec.
J_D = mass transfer factor, $k\rho/G$, dimensionless
k = mass transfer coefficient across external gas film, cm./sec.
K_E = external mass transport property, kav_t/F, dimensionless
K_I = internal mass transport property, $4\pi\alpha D\tau r_E v_t/F$, dimensionless
m = finite difference increment designation for V
n = amount of reacting fluid which has reacted in the pellet phase, g.-moles/cc. of bed
n = finite difference increment designation for ZV
N_{Re} = modified Reynolds number, $d_P G/\mu$, dimensionless
N_{Sc} = Schmidt number, $\mu/D\rho$, dimensionless
r = radial distance within spherical particle, cm.
R = radial distance within spherical partcle, r/r_E, dimensionless
t = time, sec.
u = interstitial fluid velocity, cm./sec.
U = linearized pellet-phase fluid concentration, $C_s \cdot r$, g.-mole/sq.cm.
v = bed volume in column from gas entrance to a distance of z, cc.
V = bed volume in column up to a column height of z, v/v_t, dimensionless
X = fluid phase concentration, C/C_o, dimensionless
Y = pellet reacted phase concentration, $3n/(4\pi r_E^3 b\tau)$, dimensionless
z = distance in column from entrance, cm.
Z = throughput parameter, $3C_o(Ft - v\epsilon)/4\pi r_E^3 b\tau v$, dimensionless
α = effective internal pellet porosity, ratio of effective internal void volume to total pellet volume, dimensionless
Δ = difference
ϵ = external bed porosity, ratio of void volume external to pellets to total bed volume, dimensionless
μ = viscosity of fluid, g./cm. sec.
ρ = fluid density, g./cu.cm.
τ = specific average copper oxide pellet density, pellets/cu.cm.

Subscripts

I = reaction interface within pellet
E = external surface of pellet
o = inlet
s = within pellet
t = total

LITERATURE CITED

1. Anderson, F. A., *U.S. At. Energy Comm. Rep., ORNL-2819* (1959).
2. Bond, W. D., and W. E. Clark, *ibid., ORNL-2816* (1960).
3. Bischoff, K. B., *Chem. Eng. Sci.*, **18**, 711 (1963).
4. Booth, F., *Trans. Faraday Soc.*, **44**, 796 (1948).
5. Bradshaw, R. D., and C. O. Bennett, *AIChEJ.*, **7**, 48 (1961).
6. Carberry, J. J., *ibid.*, **6**, 460 (1960).
7. Chilton, T. H., and A. P. Colburn, *Ind. Eng. Chem.*, **26**, 1183 (1934).
8. Chu, Ju Chin, H. Kalil, and W. A. Wetteroth, *Chem. Eng. Progr.*, **49**, 141 (1953).
9. Chufarov, G. I., et al., *Zhur. Fiz. Khim.*, **26**, 31 (1952).
10. Crank, J., "The Mathematics of Diffusion," chapt VI, Oxford Univ. Press, London (1956).
11. Dryden, C. E., D. A. Strang, and A. E. Withrow, *Chem. Eng. Progr.*, **49**, 191 (1953).
12. Ergun, S., *ibid.*, **48**, 227 (1952).
13. Gaffney, B. J., and T. B. Drew, *Ind. Eng. Chem.*, **42**, 1120 (1950).
14. Hedley, W. H., Ph.D. dissertation, Washington Univ., St. Louis, Mo. (1957).
15. Hermans, J. J., *J. Colloid Sci.*, **2**, 387 (1947).
16. Hobson, M., and G. Thodos, *Chem. Eng. Progr.*, **47**, 370 (1951).
17. Hoogschagen, J., *Ind. Eng. Chem.*, **47**, 906 (1955).
18. Hurt, D. M., *ibid.*, **35**, 522 (1943).
19. Kasten, P. R., L. Lapidus, and N. R. Amundson, *J. Phys. Chem.*, **56**, 683 (1952).
20. Klotz, I. M., *Chem. Review*, **39**, 241 (1946).
21. Larson, A. J., and F. E. Smith, *J. Am. Chem. Soc.*, **47**, 346 (1925).
22. Levenspiel, O., "Chemical Reaction Engineering," John Wiley, New York (1962).
23. Masamune, Shinobu, and J. M. Smith, *Ind. Eng. Chem. Fundamentals*, **3**, 179 (1964).
24. Massey, G. V., *At. Energy Res. Estab. (G. B.), Rep. 14*(D) (1960).
25. Pavlyuchenko, M. H., and Y. S. Rubinchik, *J. Appl. Chem. (USSR)*, **24**, 751 (1951).
26. Pease, R. N., and H. S. Taylor, *J. Am. Chem. Soc.*, **43**, 2179 (1921).
27. Pekeris, C. H., and L. B. Slichter, *J. Appl. Phy.*, **10**, 135 (1939).
28. Reid, R. C., and T. K. Sherwood, "The Properties of Gases and Liquids," McGraw-Hill, New York (1958).
29. Resnick, W., and R. R. White, *Chem. Eng. Progr.*, **45**, 377 (1949).
30. Rosen J. B., *Ind. Eng. Chem.*, **46**, 1590 (1954).
31. Shulman, H. L., and L. J. Delaney, *AIChEJ.*, **5**, 290 (1959).
32. Thiele, E. W., *Ind. Eng. Chem.*, **38**, 646 (1946).
33. Vermeulen, T., *ibid.*, **45**, 1664 (1953).
34. ———, "Advances in Chemical Engineering," Vol. II, pp. 147-208, Academic Press, New York (1958).
35. Villet, R. H., and R. H. Wilhelm, *Ind. Eng. Chem.*, **53**, 837 (1961).
36. Weisz, P. B., and R. D. Goodwin, *J. Catalysis*, **2**, 397 (1963).
37. Wheeler, A., "Advances in Catalysis," Vol. II, chap. 2, Reinhold, New York (1954).
38. Weight, C. R. A., and A. P. Luff, *J. Chem. Soc.*, **33**, 1 (1878).

Manuscript received February 10, 1967; revision received January 19, 1968; paper accepted January 22, 1968.